A Microscopic Basis for the Global Appearance of Energy Landscapes

David J. Wales

It is shown that the appearance of a multidimensional potential energy surface, or potential energy landscape, can be related to the form of the interatomic or intermolecular potential. Catastrophe theory enables us to describe how the geometry of the surface changes with parameters in the potential, and provides universal scaling relations that explain, for example, the asymmetric reaction profiles observed for systems bound by long-range forces. The principal result is an unexpected connection between barrier heights, path lengths, and vibrational frequencies, with applications to a wide variety of problems in chemical physics, ranging from Hammond's postulate in organic chemistry, to the relaxation dynamics of complex systems such as glasses and biomolecules.

The structure, dynamics, and thermodynamics of any system in a particular electronic state are determined by the underlying potential energy surface (PES). Considerable effort has been made to discover how the global topography of the PES enables some systems, such as proteins and crystals, to locate low-energy states reliably, whereas others readily form glasses (*1*–*8*). Of equal importance, but much less studied, is the parallel question of how the global characteristics of the PES are determined by the nature of the interatomic or intermolecular potential. This is the question considered in the present report.

A multidimensional PES can be thought of as a mountain range, where local minima are basins, and transition states correspond to the lowest passes linking valleys (*9*). The lowest energy structure is the global minimum, and this is where the system will reside at 0 K unless this point is kinetically inaccessible. Above this temperature, thermodynamic properties depend on the different local minima that the system samples as it explores the landscape dynamically, using thermal energy to overcome the potential energy barriers.

If the system is changed, by altering a functional group or some other aspect of the chemical composition, then the PES changes as well. Predicting and understanding the associated changes in physical and chemical properties is a cornerstone of molecular science. Catastrophe theory provides a mathematical description of how the PES changes with variations in any such parameter: Around points where minima and transition states disappear, the local geometry is described by certain catastrophe functions. The present results reveal that the predicted features are indeed present in the energy landscapes of molecules and solids, and that it is not necessary to specify the parameter in question for quantitative relations to be obtained.

To properly appreciate the insight that catastrophe theory provides, it may be helpful to extend the analogy with a mountain range still further. Suppose that we were somehow able to study the geography as a function of parameters such as the composition of the rocks, the rate at which they cooled, or the motion of underlying tectonic plates. Catastrophe theory requires that the local geometry at points in parameter space where basins and passes disappear must have a universal form. Now suppose instead that we survey a whole series of mountain ranges at some fixed point in time. The same geometric relation between basins, peaks, and passes must be obeyed when such features lie close together, and we expect to see increasing deviations from ideal behavior for points that are further apart.

In the context of molecular science, catastrophe theory establishes a quantitative connection between the potential energy barrier, the path length, and the lowest vibrational frequencies for a steepest-descent path linking a minimum and a transition state. This result may appear counterintuitive, for one might suppose that these quantities are independent. Catastrophe theory says otherwise, and a number of examples are presented below, illustrating that ideal relations hold in the limit of small path lengths, and that the deviations from ideality may be small enough in many cases for the results to remain useful.

Minima and transition states on a PES are both examples of stationary points where the gradient of the energy vanishes. Stationary points are further classified by their Hessian index, which is equal to the number of independent directions for which a small displacement causes the energy to decrease. The Hessian itself is the matrix of second derivatives of the energy with respect to coordinates. A minimum has index zero, because there is a restoring force for any perturbation of the structure. However, for a transition state, displacements along the reaction coordinate cause the energy to decrease, and the Hessian index is unity. The organization of the PES is determined by its stationary points, whose properties can be defined in terms of Taylor expansions in the coordinates.

The mathematical basis for catastrophe theory and the universal behavior that it predicts are more subtle (*10*, *11*). However, the basic result is an extension of the Taylor series to provide a local representation of the PES as a function of both atomic coordinates and the parameters on which the PES depends. The parameters may either be explicit, as in empirical interatomic or intermolecular potentials, or implicit, as for numerical solutions of the Schrödinger equation, which depend upon the identity of the nuclei and the choice of basis set.

If explicit or implicit parameters are varied continuously, then the organization of the resulting families of PESs is determined by the stationary points that possess additional zero eigenvalues of the Hessian matrix (*11*), beyond those required by conservation laws (*12*). These points, known as non-Morse points, separate the parameter space into regions within which the PES has the same qualitative properties. Within any such region, small changes in parameters produce correspondingly small changes in the PES. In contrast, the dividing surface between regions marks the appearance or disappearance of one or more stationary points, and the behavior in the vicinity of a non-Morse point can be written in terms of certain catastrophe functions (*10*). Catastrophe theory predicts that the geometry of any non-Morse point must fall into one of a number of universal categories. These universal properties will now be exploited to deduce some quantitative results for the properties of an atomic or molecular PES.

The form of the catastrophe function depends on the number of additional zero Hessian eigenvalues and the number of control parameters. Using a simple Morse potential (*13*) to describe the interatomic forces, we can explicitly follow the coalescence of minima-transition state pairs corresponding to elementary catastrophes. The potential energy is then

$$V = \varepsilon \sum_{i<j} e^{\rho(1-r_{ij}/r_e)}(e^{\rho(1-r_{ij}/r_e)}-2) \qquad (1)$$

where ε is the pair well depth, r_e is the pair equilibrium separation, and ρ is a parameter that governs the range of the interaction. Conventionally, the range decreases as ρ increases (*14*–*17*).

University Chemical Laboratories, Lensfield Road, Cambridge CB2 1EW, UK. E-mail: dw34@cam.ac.uk

For a single extra zero Hessian eigenvalue and a single control parameter, the local geometry when a minimum and transition state approach with changing ρ is that of a fold catastrophe (*10*, *11*), and a simple example is illustrated in Fig. 1. Catastrophe theory predicts that the reaction coordinate in this situation can be written as a cubic polynomial (*10*, *11*), and identifying coefficients with physical observables produces the key result (*18*)

$$6\Delta V/\lambda\Delta s^2 = 1 \qquad (2)$$

where ΔV is the energy difference between the minimum and the transition state, which are separated by a distance Δs. The smallest non-zero Hessian eigenvalues of the transition state and the minimum are $-\lambda$ and $+\lambda$, respectively (Fig. 2). We will henceforth refer to the quantity $6\Delta V/\lambda\Delta s^2$ as the fold ratio, denoted by r_f.

The number of possible catastrophes increases rapidly with the number of control parameters, and we have characterized one further class of catastrophe for rearrangements involving an overall change in morphology. Again, the non-Morse point in question exhibits a single extra zero Hessian eigenvalue, but this time the geometry corresponds to a cusp catastrophe (*10*, *11*). Identifying coefficients of the predicted even quartic polynomial now gives (*18*)

$$8\Delta V/\lambda\Delta s^2 = 1 \qquad (3)$$

and we now define the cusp ratio as $r_c = 8\Delta V/\lambda\Delta s^2$ (Fig. 2).

The relative powers of ΔV, λ, and Δs in both r_c and r_f could actually have been predicted by dimensional analysis. More complex catastrophes can be analyzed along similar lines, and we need not restrict ourselves to pathways between minima and transition states, nor to non-Morse points with only one extra Hessian eigenvalue. However, analysis of the databases of pathways discussed below suggests that the simplest fold catastrophe is probably the most ubiquitous.

The above cusp catastrophe describes the geometry of the PES for competition between icosahedral and close-packed clusters as a function of ρ (Fig. 1). The relative stability of the close-packed cluster increases as the range decreases, because this structure is not strained (*19*, *20*). The cuboctahedral intermediate is therefore most likely to be observable in atomic or molecular clusters where a description in terms of short-ranged isotropic forces is appropriate. The full range of behavior described by the cusp catastrophe may perhaps be realized for clusters composed of different transition metals as we move across a row of the periodic table.

For the above examples, we have verified that r_f and r_c remain close to unity for a significant range of ρ (*18*). Hence, the conditions expressed in Eqs. 2 and 3 are obeyed quite well for sufficiently small but

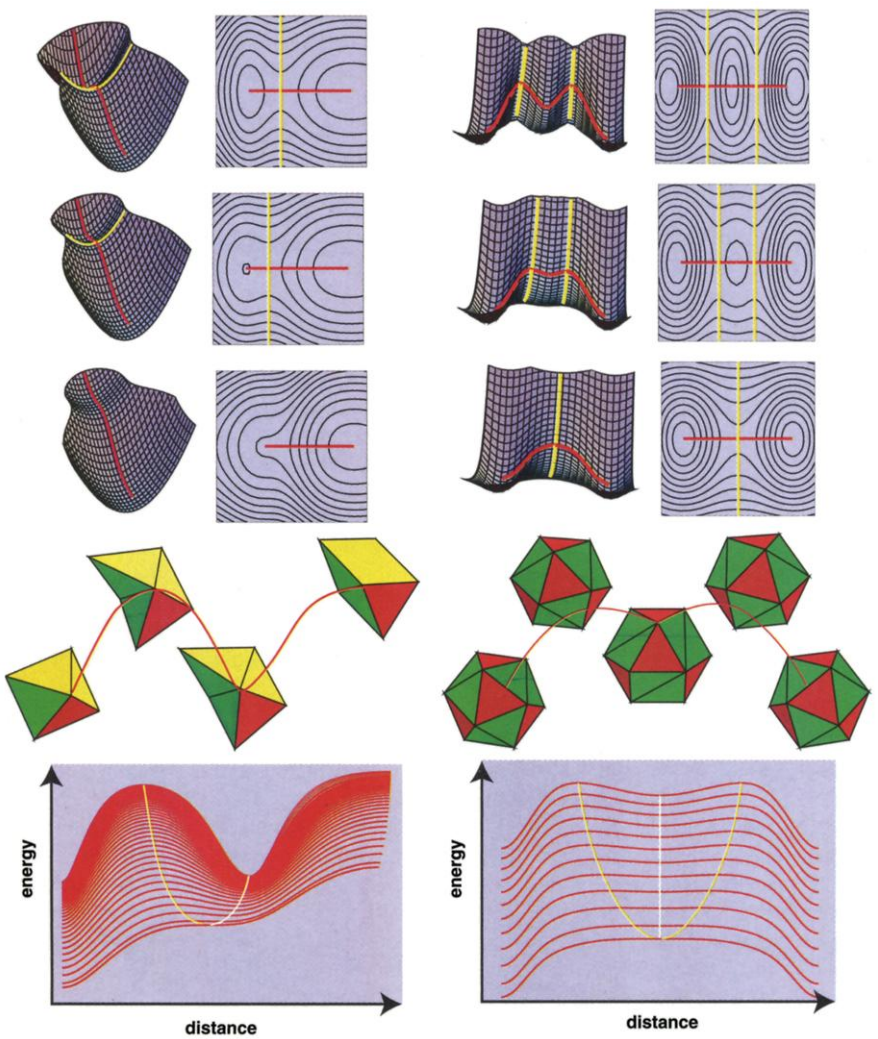

Fig. 1. Evolution of fold (**left**) and cusp (**right**) catastrophes for two clusters bound by the Morse potential. Schematic surface and contour plots are shown for three values of ρ, and a family of true steepest-descent paths calculated for each system is shown at the bottom. Steepest-descent paths are plotted in red, and dividing surfaces, including transition states, are plotted in yellow. The stationary points (minima and transition states) for a particular value of ρ are shown superimposed on one of the pathways below the surface plots. (Left) Rearrangement of a six-atom octahedral cluster. At short range (large ρ), a C_{2v} transition state links the O_h global minimum to a C_{2v} minimum, and a higher energy C_s symmetry transition state links permutational isomers of the C_{2v} minimum. The yellow and white curves indicate the position of the C_{2v} transition state and the C_{2v} minimum, respectively, as a function of ρ. At long range ($\rho < 4.098$), the C_{2v} transition state and minimum merge, and the C_s transition state links permutational isomers of the O_h minimum directly. (Right) Rearrangement of an icosahedral cluster containing 147 atoms. At short range (large ρ), a T_h symmetry transition state links the I_h global minimum to a cuboctahedral O_h minimum. The yellow and white curves indicate the position of the two T_h symmetry transition states and the O_h minimum, respectively, as a function of ρ. At long range ($\rho < 5.331$), the T_h transition state disappears and the cuboctahedron becomes a transition state directly linking two permutational isomers of the global minimum icosahedron.

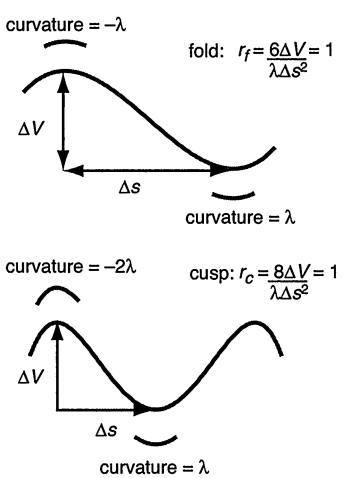

Fig. 2. Geometry of the fold and cusp catastrophes corresponding to steepest-descent paths connecting minima and transition states. ΔV is the potential energy barrier, Δs is the path length, and λ is the curvature.

finite values of ΔV and Δs. This result greatly extends the applicability of the above analysis, because it enables us to predict trends in the form of the PES. To provide a meaningful comparison between different systems, energy and distance can be measured in units of the pair well depth and separation. Systems bound by short-range potentials then have larger curvatures, and hence larger values of λ. For example, with the Morse potential, the curvature at the bottom of the well scales as ρ^2. Equations 2 and 3 both imply that the ratio $\Delta V/\Delta s^2$ increases as the range decreases, or more generally, as the curvature of the potential increases.

Short-ranged potentials lead to rough surfaces because the density of minima in the $3N$-dimensional configuration space is higher—the weaker interaction of distant regions leads to additional stable packings. As the range of the potential increases, or more generally, as the curvature of the potential decreases, λ decreases and minimum/transition state pairs are progressively eliminated by fold (or other) catastrophes. Both ΔV and Δs tend to zero as the stationary points approach, but ΔV must decrease faster than Δs^2, because the ratio is proportional to λ. This trend on its own tends to decrease both uphill and downhill barriers. However, when a minimum disappears, the steepest-descent paths that connected it to higher lying transition states must continue downhill to lower energy, and the corresponding barriers increase discontinuously. As the curvature of the potential diminishes, the net result of the steady decrease in barrier heights coupled to sudden jumps is that larger barriers and path lengths tend to grow, whereas smaller barriers and path lengths tend to shrink. These trends explain the systematic changes in reaction path profiles observed in earlier work (*7*, *21*, *22*), which are also evident in Fig. 1.

Obviously, the PES for a given physical system has a limiting form given by the exact solution of the corresponding Schrödinger equation. In experiments, it may only be possible to vary parameters discretely, such as the identity of a particular element or functional group. To investigate whether catastrophe theory is likely to be useful when the potential is fixed, r_f has been calculated for databases containing 4000 pathways each for model Ar_{19} and $Na_{35}Cl_{36}^-$ clusters. These systems were chosen because of the patterns recognized in previous work, especially the staircase profile characteristic of pathways in alkali halide clusters (*7*, *21*, *22*). The results show that r_f is correlated with Δs, and converges to unity as the path length decreases (Fig. 3). Notice that it is not necessary to specify or vary a control parameter here; the scaling properties of the catastrophe are independent of how it arises.

Three further examples illustrate the wide range of potential applications for the present theory. Relating changes of structure to changes in energetics and kinetics is a key goal of physical organic chemistry. One of the most important ideas used in analyzing such relations is Hammond's postulate (*23*), that the transition state most closely resembles the higher in energy of the products and reactants (*23*). This intuitive approach can now be placed on a firm basis using the above

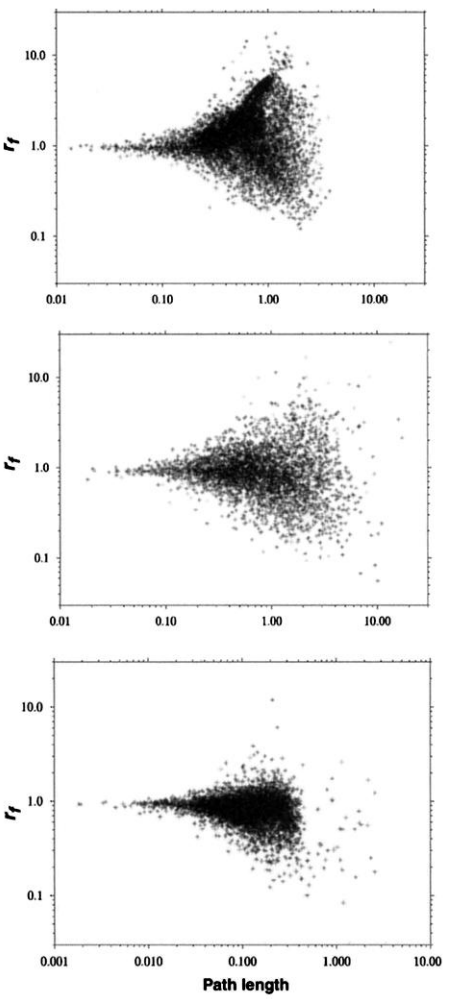

Fig. 3. Scatter plots of the fold ratio, r_f, against path length, Δs, for rearrangements of an Ar_{19} cluster (**top**), a $Na_{35}Cl_{36}^-$ cluster (**middle**), and some bulk atomic glass-formers (**bottom**). These results are all for the steepest-descent path connected to the higher energy minimum (the "downhill" path), and the plots contain 4000, 4000, and 11121 points, respectively. For the $Na_{35}Cl_{36}^-$ cluster, the path length is scaled by the NaCl equilibrium distance. The results for the bulk glass-formers were obtained from much larger databases (*31*), including pathways for four different systems modeled by supercells containing either 216 or 256 atoms. The shortest paths occur for bulk silicon modeled by the Stillinger-Weber potential (*32*); the other three systems are homogeneous and binary Lennard-Jones (*33*) models.

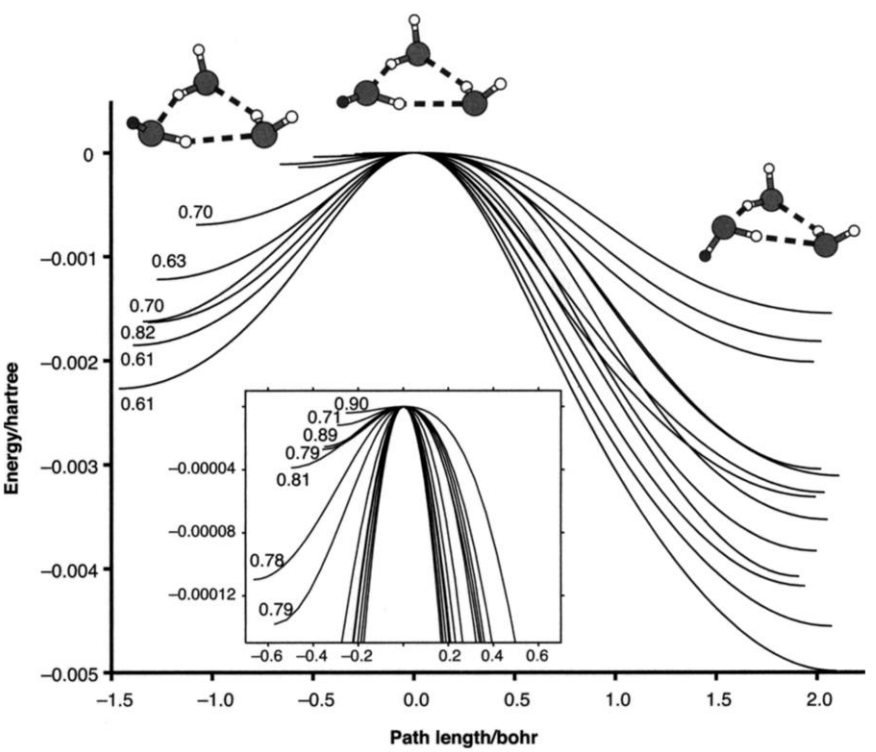

Fig. 4. Rearrangement pathways between the crown minimum (**left**) and the global minimum (**right**) of water trimer calculated at 13 levels of ab initio theory. The shaded hydrogen atom undergoes a "flip" in this process, and the origin is chosen at the transition state for both energy and path length in each case. Values of $100 \times r_f$ are given for the low-barrier side of each path, and the inset shows a magnified view of the shortest paths.

results. The smaller the downhill barrier, the closer we expect r_f to be to unity, and hence the shorter the downhill path length, i.e., the geometrical distortion from the corresponding minimum. Recent applications of this principle extend to enzyme catalysis and protein engineering. For example, correlation between the transition state structure and destabilization of the native state of chymotrypsin inhibitor 2 by mutation suggests that unfolding proceeds by way of an ensemble of related transition states (*24*). Using the present results in a more quantitative fashion, perhaps in combination with models such as Marcus theory (*25*), is a likely area of future research.

One aspect of the complex phenomenology of glasses is the appearance of anomalous heat capacities and conductivities at low temperature. It has been suggested that these properties are due to quantum tunneling between pairs of minima referred to as two-level systems (TLSs) (*26–28*). Angell (*29*) has further associated TLSs with the low-frequency excess vibrational density of states observed in many glasses, known as the "boson peak." For tunneling between two minima to be significant, they must be separated by a low, narrow barrier, which suggests that the present theory may apply. Results are shown in Fig. 3 for more than 10^4 pathways calculated for several bulk model atomic glass-formers, as described in detail elsewhere (*30*). This database contains a number of very short paths, and we see that these do indeed have $r_f \approx 1$. The asymmetric "staircase" profile now established for long-range interactions above is expected to produce more efficient local relaxation to low-energy structures. However, this observation in itself is not sufficient to predict the glass-forming propensity, which depends on longer-ranged correlations between features of the PES.

High-resolution spectroscopy has recently provided detailed insight into the dynamics of weakly bound complexes, particularly water clusters (*31*), and has inspired much theoretical work. The present theory is equally applicable to small molecules, and results are presented in Fig. 4 for pathways between the "crown" and global minimum geometries of $(H_2O)_3$, calculated ab initio with various different basis sets and treatments of the correlation energy. Again, we see that r_f is close to unity for the low-barrier side of the path, and the ratio is generally nearer to its ideal value for the shortest path lengths. It may be possible to exploit such results in quantum dynamics calculations and analysis of intermolecular forces.

Correlations between structure, dynamics, and thermodynamics are important throughout molecular science. The present results provide new tools to tackle such problems, with a wide range of possible applications.

References and Notes

1. P. E. Leopold, M. Montal, J. N. Onuchic, *Proc. Natl. Acad. Sci. U.S.A.* **89**, 8721 (1992).
2. J. D. Bryngelson, J. N. Onuchic, N. D. Socci, P. G. Wolynes, *Proteins* **21**, 167 (1995).
3. P. G. Wolynes, J. N. Onuchic, D. Thirumalai, *J. Chem. Phys.* **102**, 1619 (1995).
4. C. A. Angell, *Science* **267**, 1924 (1995).
5. F. H. Stillinger, *Science* **267**, 1935 (1995).
6. J. P. K. Doye, D. J. Wales, *J. Chem. Phys.* **105**, 8428 (1996).
7. K. D. Ball, R. S. Berry, R. E. Kunz, F. Y. Li, A. Proykova, D. J. Wales, *Science* **271**, 963 (1996).
8. N. D. Socci, J. N. Onuchic, P. G. Wolynes, *Proteins Struct. Funct. Genet.* **32**, 136 (1998).
9. P. G. Mezey, *Potential Energy Hypersurfaces* (Elsevier, Amsterdam, 1987).
10. R. Thom, *Stabilité Structurelle et Morphogénèse* (Benjamin, New York, 1972).
11. R. Gilmore, *Catastrophe Theory for Scientists and Engineers* (Wiley, New York, 1981).
12. Stationary points of molecular systems possess zero eigenvalues when the energy is invariant with respect to overall translation or rotation.
13. P. M. Morse, *Phys. Rev.* **34**, 57 (1929).
14. P. A. Braier, R. S. Berry, D. J. Wales, *J. Chem. Phys.* **93**, 8745 (1990).
15. J. P. K. Doye, D. J. Wales, *J. Chem. Soc. Faraday Trans.* **93**, 4233 (1997).
16. M. A. Miller, J. P. K. Doye, D. J. Wales, *J. Chem. Phys.* **110**, 328 (1999).
17. ———, *Phys. Rev. E* **60**, 3701 (1999).
18. More details are given in the supplementary material available on *Science* Online at www.sciencemag.org/cgi/content/full/293/5537/2067/DC1.
19. J. P. K. Doye, D. J. Wales, *J. Phys. B* **29**, 4859 (1996).
20. ———, *Science* **271**, 484 (1996).
21. R. S. Berry, N. Elmaci, J. P. Rose, B. Vekhter, *Proc. Natl Acad. Sci. U.S.A.* **94**, 9520 (1997).
22. D. J. Wales, J. P. K. Doye, M. A. Miller, P. N. Mortenson, T. R. Walsh, *Adv. Chem. Phys.* **115**, 1 (2000).
23. G. S. Hammond, *J. Am. Chem. Soc.* **77**, 334 (1955).
24. A. Fersht, *Structure and Mechanism in Protein Science* (Freeman, New York, 1999).
25. R. A. Marcus, *Annu. Rev. Phys. Chem.* **15**, 155 (1964).
26. P. Anderson, B. Halperin, C. Varma, *Philos. Mag.* **25**, 1 (1972).
27. W. Phillips, *J. Low Temp. Phys.* **7**, 351 (1972).
28. R. Zeller, R. Pohl, *Phys. Rev. B* **4**, 2029 (1971).
29. C. A. Angell, *J. Phys. Condens. Matter* **12**, 6463 (2000).
30. T. F. Middleton, D. J. Wales, *Phys. Rev. B* **64**, 024205 (2001).
31. K. Liu, J. D. Cruzan, R. J. Saykally, *Science* **271**, 929 (1996).
32. F. H. Stillinger, T. A. Weber, *Phys. Rev. B* **31**, 5262 (1985).
33. S. Sastry, P. G. Debenedetti, F. H. Stillinger, *Nature* **393**, 554 (1998).

34. This paper is dedicated to R. S. Berry on the occasion of his 70th birthday. I am grateful to J. Kobine for discussions concerning catastrophe theory, and to J. Doye and A. Kirby for helpful comments.

16 May 2001; accepted 2 August 2001

Active Normal Faulting in the Upper Rhine Graben and Paleoseismic Identification of the 1356 Basel Earthquake

Mustapha Meghraoui,[1]* Bertrand Delouis,[2] Matthieu Ferry,[2] Domenico Giardini,[2] Peter Huggenberger,[3] Ina Spottke,[3] Michel Granet[1]

We have identified an active normal fault in the epicentral area of the Basel (Switzerland) earthquake of 18 October 1356, the largest historical seismic event in central Europe. The event of 1356 and two prehistoric events have been characterized on the fault with geomorphological analysis, geophysical prospecting, and trenching. Carbon-14 dating indicates that the youngest event occurred in the interval 610 to 1475 A.D. and may correspond to the 1356 Basel earthquake. The occurrence of the three earthquakes induced a total of 1.8 meters of vertical displacement in the past 8500 years for a mean uplift rate of 0.21 millimeters per year. These successive ruptures on the normal fault indicate the potential for strong ground movements in the Basel region and should be taken into account to refine the seismic hazard estimates along the Rhine graben.

To understand the damage produced by past earthquakes and to forecast future earthquake scenarios, an analysis of potentially active faults and related seismogenic behavior is required. An earthquake on 18 October 1356 destroyed the city of Basel, Switzerland, and damaged large parts of the upper Rhine graben (Fig. 1). This large earthquake had an epicentral intensity of IX to X on the MSK scale (*1*) and an estimated magnitude of 6.0 to 6.5 (*2*, *3*). Thirty to 40 castles were destroyed within a 10-km radius around Basel, and castles, towers, and churches within a 200-km radius were damaged (*2*, *3*) (Fig. 2). The Basel region belongs to an area with a low seismicity level and a long seismic cycle. Basic knowledge on seismogenic faults in this area is lacking, and the hazards evaluation depends on the sporadic occurrence of large earthquakes. To determine the activity and recurrence rate of earthquakes near Basel, we need, first, to identify the fault